[9] A. M. K. Saad and Schünemann, "Design of fin-line tapers, transitions, and couplers," in *Proc. 11th Eur. Microwave Conf.*, (Amsterdam, The Netherlands), 1981, pp. 305–308.
[10] L. Solymar, "Spurious modes in nonuniform waveguides," *IRE Trans. Microwave Theory Tech.*, vol. MTT-7, pp. 379–383, July 1959.
[11] Ch. P. Womack, "The use of exponential transmission lines in microwave components," *IRE Trans. Microwave Theory Tech.*, vol. MTT-10, pp. 124–132, Mar. 1962.

Phase-Matched Waveguide Using the Artificial Anisotropic Structure and its Application to a Mode Converter

TETSUYA MIZUMOTO, STUDENT MEMBER, IEEE, HIROHIKO YAMAZAKI, AND YOSHIYUKI NAITO, SENIOR MEMBER, IEEE

Abstract — **Phase matching by the artificial anisotropic structure and its application to a mode converter are proposed for millimeter-wave dielectric circuitry. A phase-matched dielectric planar waveguide is designed and mode conversion characteristics are studied. An experimental result of the nonreciprocal mode converter are presented to show the usefulness of the structure.**

I. Introduction

As a transmission medium for low-cost integrated circuitry, dielectric waveguides have been studied in the millimeter-wave frequency range. Couplers and filters were designed in dielectric waveguide forms and realized with good performances [1], [2]. Nonreciprocal devices, such as isolators and circulators, were also studied [3]. As the waveguiding property of dielectric waveguides in millimeter-wave frequencies is very similar to that in optical frequencies, some devices in dielectric waveguide forms are interesting for optical integrated circuits.

There has been proposed an optical isolator making use of mode conversion between two cross-polarized modes [4], [5]. In order to obtain sufficient mode coupling in these devices, it is necessary to realize phase matching between the modes in question. This means that the propagation velocities in the waveguide must be equalized. This also gives rise to a great difficulty for realizing a practical device.

In this paper, as a simulation to optical applications, we propose a method for equalizing the propagation constants of the two cross-polarized modes in a dielectric waveguide. The proposed waveguide (Fig. 1) is called an artificial anisotropic waveguide. This technique can be applied with no difficulty to waveguide-type mode converters and/or isolators. A similar waveguide has been proposed and designed for optical applications [6]. The optical artificial anisotropic waveguide consists of dielectric thin film loaded by dielectric strips. In the proposed waveguide for millimeter-wave, dielectric strips are replaced by thin conductor strips, for a conductor can be regarded as a dielectric of infinite permittivity in this frequency range.

We first describe an analytical procedure to calculate the propagation velocity in the artificial anisotropic waveguide and show an example of a design of phase-matched waveguide. Mode conversion characteristics are also examined numerically for the waveguide containing magnetic anisotropy. Finally, the mode conversion observed in a fabricated waveguide is reported.

Manuscript received June 14, 1984; revised September 4, 1984.
The authors are with the Department of Electrical and Electronic Engineering, Tokyo Institute of Technology, 2-12-1 Ookayama, Meguro-Ku, Tokyo, 152 Japan.

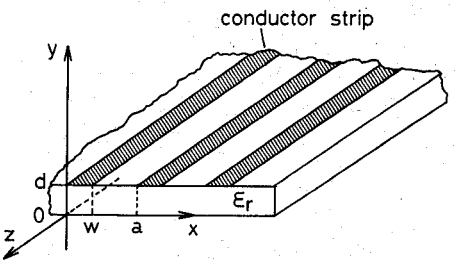

Fig. 1. The artificial anisotropic waveguide for millimeter-waves.

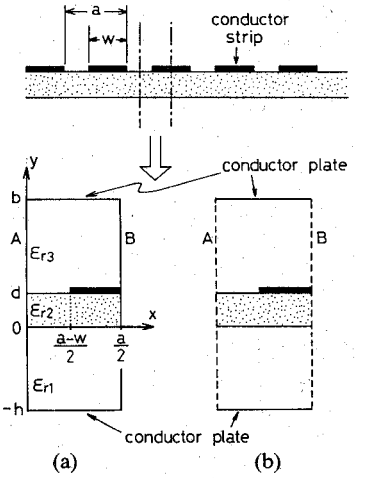

Fig. 2. Cross-sectional view of the artificial anisotropic waveguide and the structures to be analyzed. Both the planes A and B are electric walls in (a) and magnetic walls in (b).

II. Phase-Matching Condition and Mode Conversion Characteristics

Fig. 1 shows the proposed waveguide structure, which consists of a dielectric slab of thickness d loaded by conductor strips of width w. The structure extends infinitely in the $x-z$ plane. The propagation direction is along the z axis. All the materials of the waveguide are assumed to be lossless. The dielectric has a relative dielectric constant ϵ_r.

Propagating electromagnetic fields are numerically analyzed by using a method similar to that described in [7]. For simplicity of analysis, the conductor strips loading the guiding layer are placed periodically in the x direction. The periodicity is not necessary for the operating principle. For the electromagnetic fields to satisfy the periodicity in the x direction, transverse boundary conditions are restricted to the two types as shown in Fig. 2. In Fig. 2 (a), both the planes A and B are electric walls and in (b) magnetic walls. The eigenmodes can be classified into two groups, corresponding to the boundary conditions of Fig. 2(a) or (b). The former determines E^x modes and the latter E^y modes. Hypothetical conductor plates are placed at $y=-h$ and b for convenience of analysis.

When the scalar potentials for TM and TE waves are defined by $\psi^{(e)}$ and $\psi^{(h)}$, respectively, the electromagnetic fields of hybrid modes, which actually propagate in the waveguide, are given by [7, eq. (1)].

After applying the boundary conditions on both the hypothetical conductor plates and the side walls, one obtains the scalar

0018-9480/85/0002-0149$01.00 ©1985 IEEE

potential as follows:

$$\psi_1^{(ex)} = \sum_{n=1}^{\infty} A_n^{(ex)} \sinh\{\alpha_n^{(1)}(y+h)\} \sin(a_n x) \tag{1a}$$

$$\psi_2^{(ex)} = \sum_{n=1}^{\infty} \{B_n^{(ex)} \sinh(\alpha_n^{(2)} y) + C_n^{(ex)} \cosh(\alpha_n^{(2)} y)\} \sin(a_n x) \tag{1b}$$

$$\psi_3^{(ex)} = \sum_{n=1}^{\infty} D_n^{(ex)} \sinh\{\alpha_n^{(3)}(b-y)\} \sin(a_n x) \tag{1c}$$

$$\psi_1^{(hx)} = \sum_{n=0}^{\infty} A_n^{(hx)} \cosh\{\alpha_n^{(1)}(y+h)\} \cos(a_n x) \tag{1d}$$

$$\psi_2^{(hx)} = \sum_{n=0}^{\infty} \{B_n^{(hx)} \cosh(\alpha_n^{(2)} y) + C_n^{(hx)} \sinh(\alpha_n^{(2)} y)\} \cos(a_n x) \tag{1e}$$

$$\psi_3^{(hx)} = \sum_{n=0}^{\infty} D_n^{(hx)} \cosh\{\alpha_n^{(3)}(b-y)\} \cos(a_n x) \tag{1f}$$

for E^x modes, and

$$\psi_1^{(ey)} = \sum_{n=0}^{\infty} A_n^{(ey)} \sinh\{\alpha_n^{(1)}(y+h)\} \cos(a_n x) \tag{1g}$$

$$\psi_2^{(ey)} = \sum_{n=0}^{\infty} \{B_n^{(ey)} \sinh(\alpha_n^{(2)} y) + C_n^{(ey)} \cosh(\alpha_n^{(2)} y)\} \cos(a_n x) \tag{1h}$$

$$\psi_3^{(ey)} = \sum_{n=0}^{\infty} D_n^{(ey)} \sinh\{\alpha_n^{(3)}(b-y)\} \cos(a_n x) \tag{1i}$$

$$\psi_1^{(hy)} = \sum_{n=1}^{\infty} A_n^{(hy)} \cosh\{\alpha_n^{(1)}(y+h)\} \sin(a_n x) \tag{1j}$$

$$\psi_2^{(hy)} = \sum_{n=1}^{\infty} \{B_n^{(hy)} \cosh(\alpha_n^{(2)} y) + C_n^{(hy)} \sinh(\alpha_n^{(2)} y)\} \sin(a_n x) \tag{1k}$$

$$\psi_3^{(hy)} = \sum_{n=1}^{\infty} D_n^{(hy)} \cosh\{\alpha_n^{(3)}(b-y)\} \sin(a_n x) \tag{1l}$$

for E^y modes, where

$$a_n = \frac{2n\pi}{a}$$

$$\alpha_n^{(i)} = \sqrt{a_n^2 + \beta^2 - k_i^2},\ k_i = \omega\sqrt{\epsilon_0\mu_0}\sqrt{\epsilon_{ri}}, \qquad (i = 1,2,3).$$

$A_n^{(ij)}$, $B_n^{(ij)}$, $C_n^{(ij)}$, and $D_n^{(ij)}$ ($i = e, h$ and $j = x, y$) are constants to be determined. The superscript x or y denotes the quantity relating to the E^x or E^y mode, respectively.

A set of homogeneous integral equations on the unknown functions $f(\xi)$ and $g(\xi)$ can be obtained by substituting the electromagnetic fields into the boundary conditions at $y = 0$ and d and using the orthogonality of sinusoidal functions

$$\sum_{n=0}^{\infty} \{P_n(\beta) F_{ne}[F(\xi)] + R_n(\beta) G_{ne}[g(\xi)]\} \cos(a_n x) = 0 \qquad \left(0 \leqslant x \leqslant \frac{a-w}{2}\right) \tag{2a}$$

$$\sum_{n=0}^{\infty} \{R_n(\beta) F_{ne}[f(\xi)] + Q_n(\beta) G_{ne}[g(\xi)]\} \sin(a_n x) = 0 \qquad \left(\frac{a-w}{2} \leqslant x \leqslant \frac{a}{2}\right) \tag{2b}$$

for E^x modes, and

$$\sum_{n=0}^{\infty} \{-P_n(\beta) F_{nm}[f(\xi)] + R_n(\beta) G_{nm}[g(\xi)]\} \sin(a_n x) = 0 \qquad \left(0 \leqslant x \leqslant \frac{a-w}{2}\right) \tag{3a}$$

$$\sum_{n=0}^{\infty} \{-R_n(\beta) F_{nm}[f(\xi)] + Q_n(\beta) G_{nm}[g(\xi)]\} \cos(a_n x) = 0 \qquad \left(\frac{a-w}{2} \leqslant x \leqslant \frac{a}{2}\right) \tag{3b}$$

for E^y modes, where

$$F_{ne}[f(\xi)] = \int_0^{a-w/2} f(\xi) \cos(a_n \xi)\, d\xi \tag{4a}$$

$$G_{ne}[g(\xi)] = \int_{a-w/2}^{\frac{a}{2}} g(\xi) \sin(a_n \xi)\, d\xi \tag{4b}$$

$$F_{nm}[f(\xi)] = \int_0^{a-w/2} f(\xi) \sin(a_n \xi)\, d\xi \tag{4c}$$

$$G_{nm}[g(\xi)] = \int_{a-w/2}^{\frac{a}{2}} g(\xi) \cos(a_n \xi)\, d\xi. \tag{4d}$$

$f(x)$ is a distribution function of the x-directed electric field on the dielectric at $y = d$ and $g(x)$ is proportional to the z-directed electric current on the boundary surface. $P_{n(\beta)}$, $Q_{n(\beta)}$, and $R_{n(\beta)}$ are the same notation in [7]. The simultaneous homogeneous integral equations (2) and (3) are numerically solved by the discretization of the integral regions to determine the propagation constant β. In actual calculations, the summation appearing in (2) and (3) are truncated by 50.

When the conductor strips are removed, the waveguide becomes an ordinary dielectric slab waveguide. Fig. 3(a) shows the propagation constants of TE_0 and TM_0 modes in the dielectric slab waveguide as a function of the slab thickness. The guiding layer has a relative dielectric constant of 15.5 and the surrounding 1.0. Frequency is 49 GHz. Propagation velocities of the two modes never coincide with each other though they approach each other as the slab becomes thicker.

Fig. 3(b) shows the propagation constants of the lowest E^x and E^y modes in the artificial anisotropic waveguide. The guiding layer has the same dielectric constant as in the Fig. 3(a), and the surrounding is air. Conductor strips of 1.2-mm width are placed on the guiding layer with periodicity of 2.0 mm. You can see clearly that the two modes are phase matched when $d = 0.72$ mm.

If the two modes are phase matched in the waveguide composed of magnetic anisotropic material like a ferrite, nonreciprocal mode conversion occurs. Mode conversion between the E^x and E^y modes can be estimated by using a perturbation method [8].

When the E^y mode enters the waveguide with the input power of $P_y(0)$ and travels along the z direction, the converted power of E^x mode, $P_x(z)$, is given by

$$\frac{P_x(z)}{P_y(0)} = \frac{1}{1 + \left(\frac{\delta}{K}\right)^2} \sin^2(\beta_c z) \tag{5}$$

where z is the propagation distance. K, δ, and β_c are defined as follows:

$$K = \left|\omega\mu_0 \int \boldsymbol{h}_2^* \cdot \Delta\mu \boldsymbol{h}_1\, dS\right| \Big/ \left(\sqrt{A_1 A_2} \cdot \beta_m\right) \tag{6a}$$

$$\delta = (\beta_1 - \beta_2 + N_{11}/A_1 - N_{22}/A_2)/(\beta_1 + \beta_2 + N_{11}/A_1 + N_{22}/A_2) \tag{6b}$$

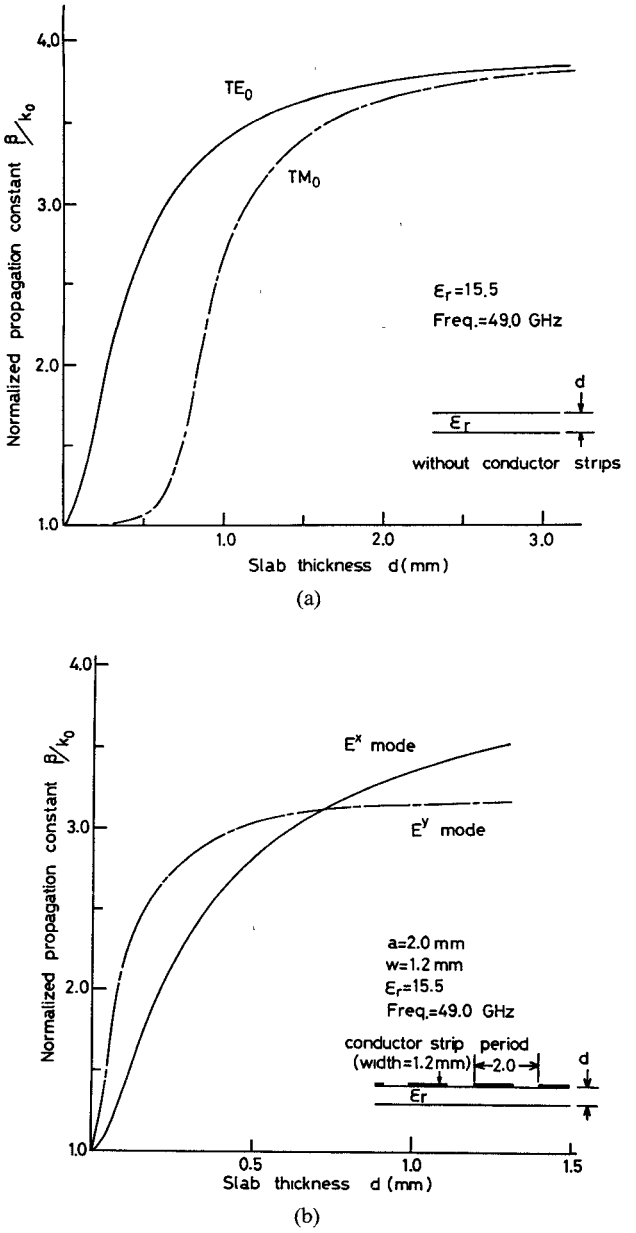

Fig. 3. Propagation constants versus slab thickness in (a) the dielectric slab waveguide and (b) the artificial anisotropic waveguide. $k_0 = \omega\sqrt{\epsilon_0\mu_0}$.

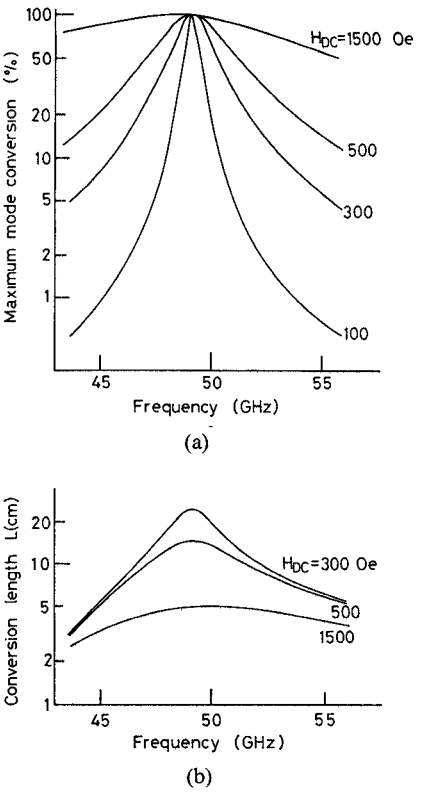

Fig. 4. Variation of (a) maximum mode conversion and (b) conversion length as a parameter of the applied dc magnetic field H_{dc}.

$$\beta_c = \beta_m K\sqrt{1+(\delta/K)^2} \tag{6c}$$

$$\beta_m = (\beta_1 + \beta_2 + N_{11}/A_1 + N_{22}/A_2)/2 \tag{6d}$$

$$N_{ii} = \beta_i + \omega\mu_0 \int \boldsymbol{h}_i^* \cdot \Delta\mu \boldsymbol{h}_i \, dS \qquad (i=1,2) \tag{6e}$$

$$A_i = \int (\boldsymbol{e}_i \times \boldsymbol{h}_i^* - \boldsymbol{h}_i \times \boldsymbol{e}_i^*) \cdot \boldsymbol{a}_z \, dS \qquad (i=1,2) \tag{6f}$$

where

$$\int dS = \int_{-h}^{b}\int_{0}^{a/2} dx\,dy.$$

β_1 and β_2 represent propagation constants of E^x and E^y modes, respectively, and $(\boldsymbol{e}_1, \boldsymbol{h}_1)$ and $(\boldsymbol{e}_2, \boldsymbol{h}_2)$ electromagnetic fields of E^x and E^y modes, respectively. $\Delta\mu$ is the tensor representing the magnetic anisotropy produced by an applied dc magnetic field

$$\Delta\mu = \begin{pmatrix} 0 & j\mu_{xy} & j\mu_{xz} \\ -j\mu_{xy} & 0 & j\mu_{yz} \\ -j\mu_{xz} & -j\mu_{yz} & 0 \end{pmatrix}. \tag{7}$$

Fig. 4 shows the maximum mode conversion

$$\frac{1}{1+\left(\frac{\delta}{K}\right)^2} \tag{8}$$

and the conversion length

$$\frac{\pi}{2\beta_c} \tag{9}$$

as a parameter of the applied dc magnetic field, i.e., the magnitude of magnetic anisotropy. The assumed waveguide consists of a ferrite slab loaded by the conductor strips of the same dimension as in Fig. 3(b). The relative dielectric constant of ferrite is 15.5 and its permeability is given by the Polder's tensor with $4\pi M_S = 1800$ (Gauss). A 100-percent conversion occurs at 49 GHz where the two modes are phase matched.

So far we have discussed a waveguide with perfectly conducting strips. In practice, however, conductor strips have finite conductivity, which might affect the mode conversion characteristics. The attenuation due to the conductor loss is estimated to the amount of several dB/m in a shielded inverted stripline at 50 GHz [9]. The change of propagation constant due to the loss in the proposed waveguide can be roughly estimated of the order of 10^{-4}, which corresponds to the frequency shift of about 0.01 GHz around 49 GHz. Thus, even if the attenuation of the E^x and E^y modes are different from each other, the phase-matching frequency shifts 0.02 percent at the most. By this frequency shift,

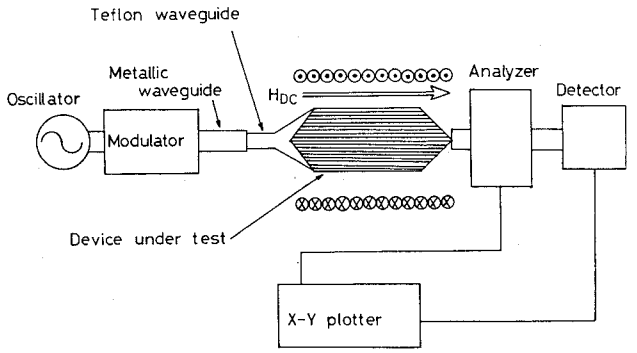

Fig. 5. Setup for measurement of polarized direction.

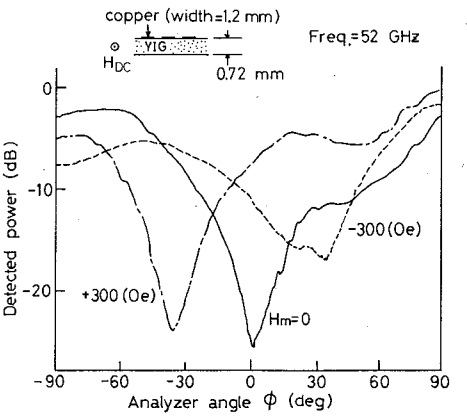

Fig. 6. Observed rotation of polarized direction.

the mode conversion is degraded only 0.04 percent at 49 GHz, when the applied magnetic field is 1500 (Oe). So far as conductor loss is concerned, insertion loss of less than 1 dB is expected for the device length of 5 cm.

III. Experimental Examination

In order to confirm experimentally our idea, we fabricated an artificial anisotropic waveguide and performed experiments on mode conversion. The fabricated waveguide consists of a YIG polycrystalline slab of 0.72-mm thickness loaded by copper strips, which are formed by etching the vacuum-evaporated copper thin film. The width and periodicity of strips are 1.2 mm and 2.0 mm, respectively. The artificial anisotropic waveguide is 5.0 cm long.

The guiding wave was launched from a metallic waveguide by way of a teflon waveguide and detected through the analyzer (Fig. 5). As is mentioned in the previous section, when the two cross-polarized modes are phase matched, nonreciprocal mode conversion occurs by virtue of magnetic anisotropy which is produced by applying a dc magnetic field parallel to the propagation direction in the YIG waveguide. This phenomenon is observed as the rotation of polarized direction (Fig. 6). In Fig. 6, the abscissa and ordinate indicate the angle of the analyzer and the detected power, respectively. Here, the polarized direction is defined as the direction making a right angle to the direction where the detected power is minimum. It is observed that the polarized direction rotates about 40 (degrees) when the applied field is 300 (Oe). On the other hand, it rotates in the reverse direction when the applied field is reversed. This means that nonreciprocal mode conversion occurred in the fabricated waveguide, as the reversal of the applied magnetic field is equivalent to that of propagation direction. Though the waveguide was designed to be phase matched at 49 GHz, the maximum mode conversion was obtained at 52 GHz. We attribute this to the fabrication errors.

We performed the same experiment on the YIG slab of the same dimension without copper strips. In this case, no mode conversion could be observed. This implies that phase matching was not taken in the YIG slab without copper strips.

It has been shown by the experimental results that the conductor strips properly placed on the dielectric slab cause phase matching between the cross-polarized modes.

IV. Conclusions

Phase matching by the use of an artificial anisotropic structure and its application to a mode converter are proposed for millimeter-wave dielectric circuitry. Phase-matched dielectric planar waveguide is designed by using a rigorous analysis. Mode conversion characteristics are also studied in the artificial anisotropic waveguide composed of a magnetic anisotropic material. Nonreciprocal mode conversion is observed in the YIG artificial anisotropic waveguide. The polarized direction rotates about 40 (degrees) when the magnetic field of 300 (Oe) is applied to the waveguide of 5.0-cm length. Therefore, it is concluded that the planar mode converter and/or isolator can be constructed in the artificial anisotropic waveguide by virtue of magnetic anisotropy.

References

[1] G. M. Lindgren, "Coupler design in open dielectric waveguide with web registration," in *IEEE Int. Microwave Symp. Dig.*, 1981, pp. 11–13.
[2] G. L. Matthaei, D. C. Park, Y. M. Kim, and D. L. Johnson, "Some dielectric-waveguide filter structure," in *IEEE Int. Microwave Symp. Dig.*, 1983, pp. 299–301.
[3] M. Muraguchi, K. Araki, and Y. Naito, "A new type of isolator for millimeter-wave integrated circuits using a nonreciprocal travelling-wave resonator," *IEEE Trans. Microwave Theory Tech.*, vol. MTT-30, pp. 1867–1873, Nov. 1982.
[4] S. Wang, M. Shah, and J. D. Crow, "Studies of the use of gyrotropic and anisotropic materials for mode conversion in thin-film optical-waveguide applications," *J. Appl. Phys.*, vol. 43, pp. 1861–1875, Apr. 1972.
[5] J. Warner, "Nonreciprocal magnetooptic waveguide," *IEEE Trans. Microwave Theory Tech.*, vol. MTT-23, pp. 70–78, Jan. 1975.
[6] T. Mizumoto and Y. Naito, "Phase matched optical dielectric waveguide using the artificial anisotropic structure," *Electron. Commun. in Japan*, vol. 66, pp. 117–125, May 1983.
[7] E. Yamashita and K. Atsuki, "Analysis of microstrip-like transmission lines by nonuniform discretization of integral equations," *IEEE Trans. Microwave Theory Tech.*, vol. MTT-24, pp. 195–200, Apr. 1976.
[8] S. Yamamoto, Y. Koyamada, and T. Makimoto, "Normal-mode analysis of anisotropic and gyrotropic thin-film waveguides for integrated optics," *J. Appl. Phys.*, vol. 43, pp. 5090–5097, Dec. 1972.
[9] D. Mirshekar-Syahkal and J. B. Davies, "Accurate solution of microstrip and coplanar structures for dispersion and for dielectric and conductor losses," *IEEE Trans. Microwave Theory Tech.*, vol. MTT-27, pp. 694–699, July 1979.

A Design Method of Bandpass Filters Using Dielectric-Filled Coaxial Resonators

MORIKAZU SAGAWA, MITSUO MAKIMOTO, AND SADAHIKO YAMASHITA, MEMBER, IEEE

***Abstract*—Design formulas for capacitively coupled bandpass filters using dielectric-filled coaxial resonators are derived and experimentally verified. The most important advantage of this filter is its ability to provide**

Manuscript received June 14, 1984; revised September 12, 1984.
The authors are with Matsushita Research Institute Tokyo, Inc., Higashimita, Tama-Ku, Kawasaki 214, Japan.

0018-9480/85/0002-0152$01.00 ©1985 IEEE